ACS APPLIED MATERIALS & INTERFACES

Research Article

www.acsami.org

# Effective Surface Functionalization of Nanocrystalline Diamond Films by Direct Carboxylation for PDGF Detection via Aptasensor

Xianfen Wang,*[,†] Yoko Ishii,[†] A. Rahim Ruslinda,[†] Masataka Hasegawa,[‡] and Hiroshi Kawarada[†]

[†]School of Science and Engineering, Waseda University, 3-4-1 Okubo, Shinjuku-ku, Tokyo 169-8555, Japan

[‡]Nanotube Research Center, National Institute of Advanced Industrial and Technology (AIST), Tsukuba Central 5, 1-1-1 Higashi, Tsukuba, Ibaraki 305-8565, Japan

**ABSTRACT:** An aptasensor was designed on a nanocrystalline diamond (NCD) surface that combined with biological recognition elements, PDGF-binding aptamers, which inherently possess high affinity to PDGF-BB proteins. Functional components such as carboxylic acids (−COOH) and amines ($-NH_2$) were directly introduced onto the NCD surface and used as probing units for immobilization of PDGF-binding aptamers. The surface coverage of different components on the NCD was analyzed by X-ray photoelectron spectroscopy (XPS) measurements, and the effects of various functionalizations on the NCD biosensor performance were investigated via fluorescence observations. The coverages of carboxyl and amine groups achieved were 12 and 23%, respectively, for the directly aminated and carboxylated NCD; however, the lower density of carboxyl groups on the functionalized surface did not deteriorate the performance of the COOH-NCD biosensor. Fluorescence investigations demonstrated comparable performance in sensitivity and selectivity for PDGF protein detection on COOH−NCD and $NH_2$−NCD biosensors. Multiple regeneration tests clearly showed that the COOH-NCD biosensor as well as the $NH_2$−NCD biosensor retained a high performance without exhibiting any noticeable degradation.

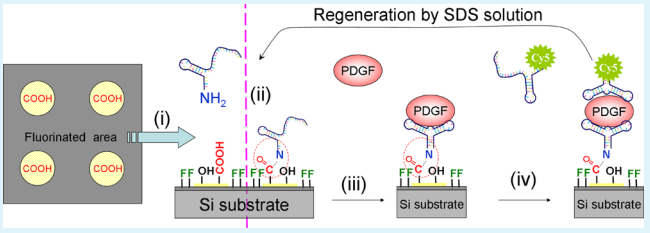


**KEYWORDS:** *nanocrystalline diamond, surface functionalization, biosensor, aptamer, PDGF*

## INTRODUCTION

Among the different types of diamond materials, nanocrystalline diamond (NCD) has been attracting increasing interest as an excellent platform for DNA immobilization and biosensing applications.[1,2] Surface functionalization is considered to be an effective approach to modulating the properties of a diamond surface by introducing diverse terminals such as −OH,[3] $-NH_2$,[1,4,5] −COOH,[2,6] and $-CF_x$ components.[7−9] Among these functionalized terminals, some have been used as tethering sites for immobilization of biomolecules onto the diamond surface.[1,2,4,6] However, because of the chemical inertness of the diamond surface, the direct modification of diamond by a versatile method of surface functionalization has been seriously impeded. Although there are various methods of surface functionalization, most of the modification strategies can require not avoid the use of linker molecules instead of modifying the diamond surface in a straightforward way when amine ($-NH_2$)[1,4] or carboxyl (−COOH)[2,6] groups are introduced onto the NCD film or diamond surface. Such surface modifications have been always carried out indirectly by using amino/carboxyl-containing linkers as tethering terminals. Furthermore, these surface functionalizations not only induce complexity in the experimental process but also inevitably impair the surface characteristic of diamond as an excellent biocompatible platform. Since diamond possesses excellent biocompatibility and stability, it is of paramount importance to establish a simple and straightforward method of introducing various types of chemical groups to enable further integrated biosensing applications. In addition, previous reports on the direct surface functionalizations of diamond for DNA immobilization have almost always been concerned with aminated diamond surfaces, and there has been very little investigation on the use of direct carboxyl groups on NCD surface for the immobilization of DNA biomolecules. Therefore, it is important to achieve the direct surface functionalization of NCD films with carboxyl and amine groups for the immobilization of DNA molecules.

Aptamers, single-stranded oligonucleotides, have been recently attracted increasing interest, because they can be selected to bind with molecular targets with high selectivity and affinity.[10] In addition, the ease with which target-binding aptamers can be selected, designed and chemically modified to contain the sequence desired and terminals makes aptamers very attractive tools for analytical biosensing applications. Therefore, aptamers have gained increasing attention among the conventional molecular recognition elements. Furthermore, aptamers are relatively stable under a wide range of conditions and can be repeatedly used without losing their binding capabilities. This further endows aptamers with high potential use for biorecognition elements.

**Received:** April 6, 2012
**Accepted:** June 14, 2012
**Published:** June 14, 2012

   dx.doi.org/10.1021/am300595f | *ACS Appl. Mater. Interfaces* 2012, 4, 3526−3534

**Scheme 1. Schematic Diagram of NCD Aptasensors for PDGF Detection via Optical Fluorescence Mode**[a]

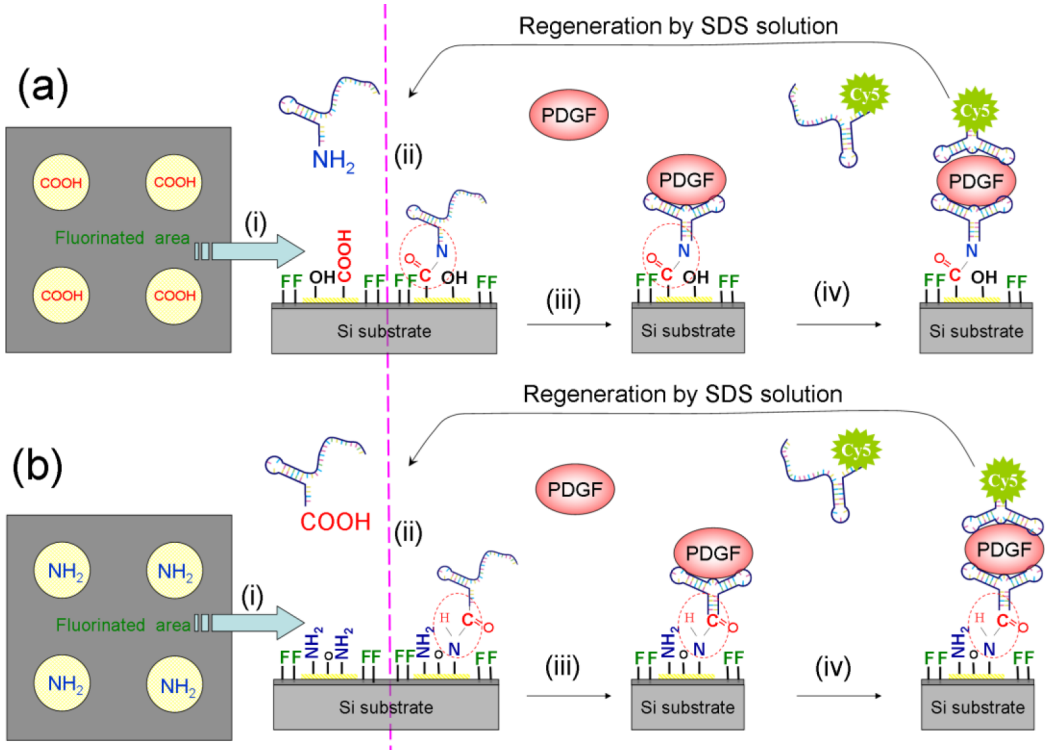


[a]Significant steps: (i) initialization of NCD biosensing surface with probe aptamers by functionalization of COOH and $NH_2$ on (a) carboxylated and (b) aminated surface, respectively; (ii) immobilization of PDGF-binding aptamers onto NCD surface; (ii) specific conjugation between introduced PDGF proteins and immobilized aptamer probes; (iii) attachment of Cy5-tagged signaling aptamer onto PDGF proteins. The regeneration cycles were achieved by thorough rinsing with SDS solution, resulting in only the probe aptamers stably immobilized on the NCD surface.

Until now, investigations comparing direct carboxylation with direct amination have not been reported on NCD surfaces, and there has been very limited study comparison of the effects of such surface functionalizations on the performance of NCD surfaces as biosensor platforms. This topic remains to be explored in detail from the view of protein detection. In this study, we attempted to achieve direct surface functionalization on NCD films with the aim of introducing covalent binding sites for the immobilization of aptamer molecules, and for the detection of platelet-derived growth factors (PDGF) protein. It is expected that the introduction of aptamers as recognition elements will open new frontiers in biosensor design on NCD platforms. A direct photochemical method was also used to introduce carboxyl or amino groups onto an NCD surface for the covalent immobilization of aptamer molecules. An optical fluorescence-based biosensor was designed by using aptamers as recognition elements for PDGF protein detection. It is highly expected that directly functionalized NCD biosensors with aptamer as biorecognition elements can be used to combine semiconductor interfaces with biomolecules.

## EXPERIMENTAL SECTION

**Materials.** NCD films were deposited using a microwave plasma chemical vapor deposition (MWPCVD) system with a low electron temperature. Prior to the deposition of NCD films, unique a novel prenucleation or seeding process was carried out that involved the ultrasonication of Si (001) substrates in adamantane-ethanol solution for 15 min.[11] This procedure is of great importance for increasing the initial density of NCD nuclei, which directly controls the quality of NCD films. For NCD deposition, a microwave power of 10−20 kW at 2.45 GHz was applied to an area with a diameter of 30 cm, and a flow of $H_2$ (90−98%)/$CH_4$ (1−5%)/CO (1−5%) was applied as a source gas for NCD deposition. The reaction gas pressure was in the range of 20−100 Pa for low-temperature NCD film growth, which is lower than that in a conventional CVD system. To avoid of the effect of static charges in XPS measurement, we have deposited a thin boron-doped layer by another MWPCVD system (Model UM-1500, Micro-DenshiGo., Ltd.) using trimethyl boron (TMB) as the doping source and 0.3% methane a B/C ratio of 6000 ppm in the hydrogen gas as the source gas during deposition.

**Surface Functionalizations.** The photochemical method was used to achieve direct surface functionalization with amine and carboxyl groups using ammonia and oxygen as source gas respectively. Direct carboxylation was carried out for 3 h in a UV/ozone cleaner (NL-UV253, Nippon Laser & Electronic Lab.) equipped with a low pressure mercury lamp (18 W, 254 nm), whereas direct amination was achieved in flowing ammonia gas for 4 h under 254 nm UV irradiation.[4] Fluorine-related groups were also introduced onto the NCD biosensor in the form of a pattern using an inductively coupled plasma reactive ion etching (ICP-RIE) system (Model RIE-101iPH; Samca International Inc., Kyoto, Japan) under typical antenna and bias powers of 500 and 20 W, respectively. $C_3F_8$ gas was introduced as a source gas of fluorine at a flow rate of 50 sccm, which resulted in a reactive chamber pressure of 5 Pa.

**Biosensor Design on NCD Surface.** The NCD biosensors were designed on the basis of the optical signals conveyed by the cy5 fluorescent dye that were tagged as the terminals of signaling aptamers. Micropatterns were fabricated via UV photolithography, resulting in an NCD surface with probing sites inside uniform dots (25 $\mu$m in diameter) for immobilizing aptamer recognition elements and a fluorinated surface in the area outside the dots (dots were separated by a distance of 25 $\mu$m). Details of the fabrication process are given elsewhere.[4] The facile surface functionalization procedure shown in Scheme 1a was conducted as follows. Direct UV irradiation was first performed to achieve COOH or $NH_2$ termination over the entire


dx.doi.org/10.1021/am300595f | ACS Appl. Mater. Interfaces 2012, 4, 3526−3534

NCD film (1.4 × 1.4 $cm^2$). This was followed by the evaporation of a protective gold film. A micropattern was then fabricated via UV photolithography, through which uniform dots were formed where the functional COOH or $NH_2$ groups were protected by the thin gold film. Finally, the area between the dots exposed to UV light during photolithography was treated with fluorine plasma, resulting in a superhydrophilic region, with the aim of suppressing nonspecific adsorption on the NCD biosensors. Therefore, the successfully fabricated biosensors on NCD films were functionalized with carboxyl or amine terminations via UV irradiation inside the dots, while the functionalization of hydrophobic fluorine was achieved via the treatment of fluorine-containing plasma. Prior to the introduction of each, thorough rinsing of the NCD biosensor was conducted via ultrasonication in acetone and distilled deionized (DI) water for 5 min each, followed by drying under flowing nitrogen gas.

Three processes are of vital importance in constructing a biosensor on NCD surface as schematically shown in Scheme 1. After effective surface functionalization, the NCD surface was covered with COOH and $NH_2$ groups as shown in a and b, respectively. The surface was modified by functionalization with a variety of groups via the formation of a micropattern.[4] Therefore, for biosensor fabrication, the NCD surface was functionalized with amino or carboxyl groups inside the dots and fluorine outside the dots as shown in step i. The biosensor fabrication begins with the effective immobilization of probing aptamers onto the NCD surface in step ii. The functionalized carboxyl or amine groups inside the dots on the NCD surface were activated to form an NHS-ester intermediate after incubation with 20 $\mu$M PDGF-binding aptamer solution containing saline-sodium citrate buffer (2 × SSC), 0.1 M N-hydroxysuccinimide (NHS), and 0.4 M 1-ethyl-3-(3-dimethylaminepropyl) carbodiimide hydrochloride (EDC) (probe in 2SSC: EDC: NHS = 2:1:1). After incubation for 2 h at 38 °C in a humidified chamber, sufficient to rinsing to remove any residual chemicals was performed using phosphate buffer solution (PBS) with Tween-20 (PBS: 1 mM, NaCl: 2 mM, $NaH_2PO_4$: 8 mM, $Na_2HPO_4$; 0.1% Tween-20) for 5 min which was followed by rinsing in DI water three times for 3 min each. Next, the biological conjugation between targeting PDGF proteins and PDGF-binding aptamers was performed for 1 h at room temperature. This resulted in the introduction of PDGF proteins with a range of concentrations onto the probing aptamers immobilized on the NCD surface. Thorough cleaning was carefully carried out in PBSM (PBS, 10 mM $MgCl_2$, pH 7.2) for 7 min. The final step was the binding of the signaling aptamers with Cy5 terminals onto the NCD biosensors for 1 h at room temperature. The regeneration procedure was performed via thorough rinsing with 10% sodium dodecyl sulfate (SDS) solution for 30 min. The conjugated PDGF proteins together with the Cy5 labeled aptamers were thus removed, resulting in only the probe aptamers stably immobilized on the NCD surface as in step ii.

**Characterization.** The morphology of the direct functionalized NCD surface was characterized by field-emission scanning electron microscopy (S-4800, JEOL, Ltd., Tokyo, Japan). Quantitative analysis of the various groups functionalized on the NCD surface after direct functionalization was performed via XPS Ulvac Φ 3300 (Ulvac-Phi, Kanagawa, Japan) with a monochromatized Al K$\alpha$ X-ray source. The electron takeoff angle (TOA) was 45 ± 3° relative to the substrate surface after focusing the monochromator radiation on the sample. The slit width (1.1 mm) and TOA were kept constant for each of the measured samples to allow each to be probed at the same depth. The pass energy was 89.5 eV for wide survey spectra and 37.5 eV for high-resolution C 1s spectra. Multipac software provided with the instrument was used to deconvolute the constituent C 1 s peaks and to integrate peak areas. The intrinsic sensitivity factors of carbon (0.30), nitrogen (0.48), oxygen (0.71), and fluorine (1.0) were used to calculate the corresponding atomic ratios from their binding energies. Surface wettability was analyzed via static contact angle measurement against water ($H_2O$) using a FACE measurement and analysis system (FAMAS). Before the contact angle measurement, all sample surfaces were thoroughly rinsed with DI water and dries with flowing nitrogen gas. The biosensor performance was evaluated using an epi-fluorescence microscope (Olympus IX71, Tokyo, Japan).

**Biological Chemicals.** All biological chemicals were purchased from Sigma Genosys (Hokkaido, Japan), including glucose oxidase, calmodulin, urease, bovine serum albumin (BSA), PDGF-binding aptamer, and PDGF isoforms such as PDGF-AB heterodimers, PDGF-AA and PGDF-BB homodimers. The sequences of probing and signaling aptamers used are listed in Table 1. Two types of probing aptamer were used with the same sequence but different terminals at the 5′ end for the carboxyl and amine groups. The signaling PDGF-binding aptamer was tagged with Cy5 fluorescent dye at the 3′ end. All chemicals were of analytical reagent grade and used without further purification.

**Table 1. Sequence of Aptamers Used for Aptasensor on Aminated and Carboxylated NCD Surfaces**

| aptamer type | sequence |
|---|---|
| PDGF-binding aptamer | NH2-5′-CAG GCT ACG GCA CGT AGA GCA TCA CCA TGA TCC TG-3′ |
| | COOH-5′-CAG GCT ACG GCA CGT AGA GCA TCA CCA TGA TCC TG-3′ |
| Cy5-tagged aptamer | Cy5-5′-CAG GCT ACG GCA CGT AGA GCA TCA CCA TGA TCC TG-3′ |

## RESULTS AND DISCUSSION

**Scanning Electron Microscopy.** Figure 1 shows typical surfaces of NCD films with a uniform morphology over the entire NCD film. Individual grains can be clearly recognized with an average size in the range of 20−30 nm. However, no well-defined crystalline facets can be observed owing to the nanosize crystalline grains. The continuous smooth film was estimated to have a thickness 110 nm with a root-mean-square (rms) roughness of approximately 10−15 nm. No rounded features or aggregated clusters of nanodiamond grains impair the film quality. However, regardless of the types of surface functionalization types of carboxylation or amination, no particular morphological changes were detected between different NCD films in the SEM observations. This lack of difference in the NCD morphology is strongly related to two facts: one is that NCD films consist of chemically inert diamond with a hybridized $sp^3$ network; and the other is that the direct carboxylation and amination of the NCD films under UV irradiation with different flowing gases were conducted under moderate condition, without introducing any deterioration associated in the film quality. The consistency of the surface morphology can be used to confirm the films with the same condition after surface modification for further biosensing applications.

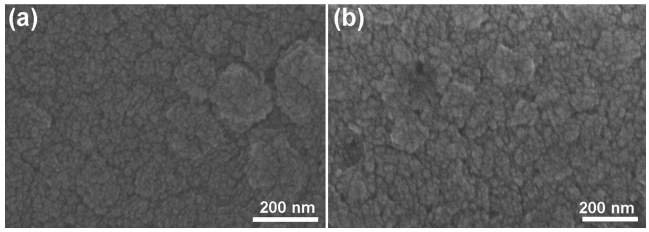


**Figure 1.** Surface morphology of NCD films after direct (a) carboxylation and (b) amination.

**X-ray Photoelectron Spectroscopy.** The XPS wide-survey spectra in Figure 2 revealed the elemental compositions on the NCD films after direct functionalization of the surface, such as those of hydrogenated NCD surface and the NCD

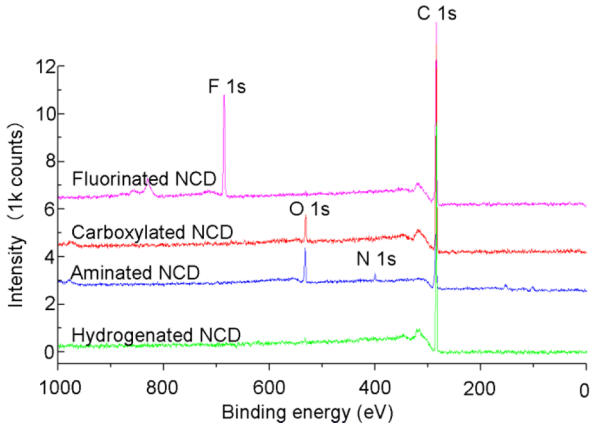


**Figure 2.** XPS survey spectra of directly functionalized NCD surfaces. In each spectrum, the C 1s signal has been normalized to the same intensity to facilitate thecomparison of the spectra.

surface after direct oxidation, amination, and $C_3F_8$ plasma fluorination. The wide spectra clearly confirm that the hydrogenated NCD surface consists of only carbon and an insignificant amount of oxygen. In contrast, both the UV/ozone-treated and photochemically aminated NCD surfaces show appreciable oxygen peaks in addition to the C 1s peaks. For the aminated NCD surface, the oxygen peak has a higher intensity than the nitrogen peak. This interesting phenomenon can also be related to the significant role of oxygen in effective amination on the NCD surface.[5] Although the exact functionalization processes remain unclear, oxygen is believed to play a crucial role in direct surface amination by increasing the grafting efficiency.[12] The wide XPS survey reveals oxygen peaks for both the directly oxidized and aminated NCD surfaces. N 1s and F 1s peaks were obtained for the aminated and fluorinated NCD surfaces, respectively. All the C 1s peaks in the spectra have been normalized to the same intensity to facilitate their direct comparison with other peaks, and a clear difference can be seen between the results of functionalization by different processes.

Figure 3 shows the core−electron C 1s spectra of NCD films after hydrogenation, UV/ozone oxidation, photochemical amination, and $C_3F_8$ plasma fluorination. The hydrogenated NCD surface shows a peak corresponding to bulk diamond with a narrow full width at half-maximum (fwhm). For the oxidized and aminated NCD surfaces, the fwhm is much wider and the spectra have a broad shoulder extending to a higher binding energy, which can be attributed to the oxygen-related functional groups labeled in the deconvoluted C 1s peaks. For the hydrogenated NCD surface, there is a special component at a lower binding energy than that of the bulk C peak. An additional investigation was performed on each NCD surface after functionalization by recording the O 1s spectra as shown in Figure 4a, in which an oxygen peak was obtained with a low

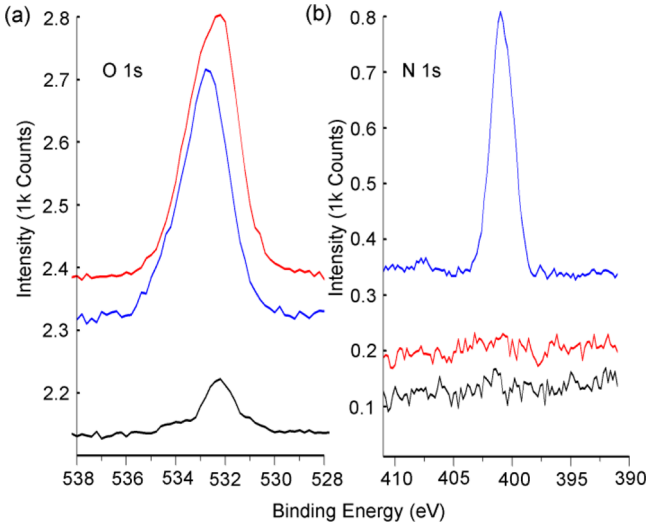


**Figure 4.** High-resolution O1 s and N 1s spectra obtained from the NCD surface after surface functionalization by hydrogenation (black), amination (blue), and oxidation (red).

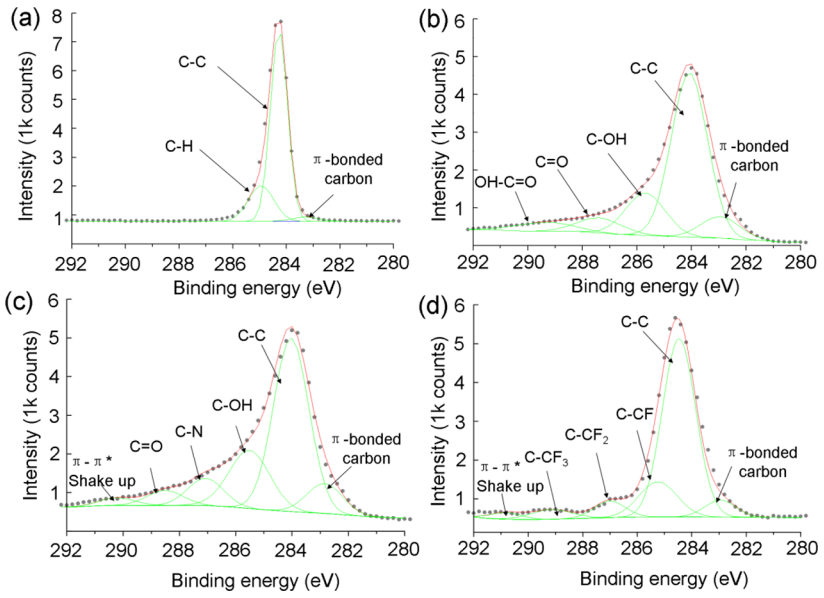


**Figure 3.** XPS C 1s high-resolution spectra showing various components on NCD surface via different functionalization treatments, (a) hydrogenation, (b) UV/ozone oxidation, (c) photochemical amination, (d) $C_3F_8$ plasma fluorination.


dx.doi.org/10.1021/am300595f | ACS Appl. Mater. Interfaces 2012, 4, 3526−3534

intensity for the hydrogenated NCD surface. Since sufficient hydrogenation was carried out in hydrogen plasma for 30 min, the outermost part of the NCD surface is assumed to have been modified by the introduction of hydrogen terminals. The oxygen species existing on the hydrogenated surface can be highly attributed to the physioadsorbed oxygen after several days of exposure to air. No treatment was performed to remove the physioadsorbed oxygen before XPS measurement. Furthermore, oxygen components may also exist as non-diamond species around grain boundaries in the NCD films.[13,14] Therefore oxygen components clearly exist on the hydrogenated NCD surface, which we tentatively assigned to $\pi$-bonded carbon atoms in the NCD films placing at a lower binding energy than that of the bulk C 1s.[5]

Compared with the hydrogenated NCD surface, both the oxidized and aminated surfaces display a clearly increased intensity in the O 1s spectra as shown in Figure 4a. The oxidized NCD surface exhibited a much heavier density of oxygen-related components, confirming the effectiveness of UV/ozone treatment in functionalizing the NCD surface. The deconvoluted C 1s peak in Figure 3b provides much more detailed information on the percentage of the various types of oxygen-related components. The proportion of defective components in the oxidized NCD film was larger than the hydrogenated NCD surface. We tentatively attributed this to the effects of the long-time UV/ozone treatment of the NCD surface, which is much more reactive and has a large number of grain boundaries. However, the directly aminated NCD surface also exhibits oxygen components, which are unexpected but may play an important role in the direct amination. A vacuum was not formed in the preparation chamber prior to the introduction of ammonia gas, but nitrogen gas was introduced to expel any residual gas in the chamber. Therefore a small mount of oxygen may still retained in the chamber at the start step for direct amination, in which oxygen may play an important role.[14] Additionally, no annealing treatment was performed to remove the physioadsorbed oxygen on the hydrogenated diamond surface. It is highly possible that these physioadsorbed oxygen components exist on the NCD surface. Furthermore, it is likely that nondiamond components around the grain boundaries in the NCD films contain some oxygen. Therefore, an atmosphere containing ozone may have been induced in the chamber, and oxygen related components were also attached onto the aminated NCD surface as a result. In addition, the reactive grain boundaries are effective for the grafting of amino groups under UV irradiation. The deconvoluted C 1s peak[15] in Figure 3c and N 1s spectra in Figure 4 reveals that nitrogen-related amine groups have been effectively attached to the NCD surface via direct photochemical amination. In addition, the amounts of nondiamond components were also markedly increased due to the high reactivity of grain boundaries, and the amounts of these species were closely related to the time of UV treatment. Although the C−N bonds show a similar amount in this case, it is difficult to draw any exact conclusions regarding the relationship between these two components, which requires further investigation. However, it is highly probable that the defective components play an important part in the surface functionalizations.

Exposure to plasma including fluorine is a very powerful surface treatment for introducing not only isolated fluorine atoms but also -$C_xF_y$ units, which result from the formation of radicals upon bond cleavage.[16−19] As shown in Figure 3d, the C 1s peak of the fluorinated surface can be deconvoluted into several fluorine-related polymer groups including C−F, C−$F_2$, and C−$F_3$. These different types of carbon−fluorine components are of great significance for chemical sensing and electronic applications. Because of the difference in electronegativity between carbon (2.5) and fluorine (4.0), strong surface dipoles exist on the fluorinated surface. As a result, the fluorinated diamond surface possesses an extremely superhydrophobic property, leading to the decreased adsorption strength of ions and molecules. In addition, a fluorinated diamond surface has also been demonstrated to be a useful termination for modulating the electrochemical properties of boron-doped diamond, leading to a lower electronic barrier than that of the hydrogenated surface.[19]

The coverage of functionalized groups was calculated basing on the deconvolution of the core-level C 1s peak, and the oxygen/carbon atomic ratios on the functionalized NCD surfaces are shown in Table 2. Note that the hydrogenated NCD surface also included a small portion of oxygen atoms (2.2%), which may be related to the $\pi$-bonded carbon atoms in nondiamond $sp^2$ components at the grain boundaries of NCD films. For the UV/ozone oxidized NCD surface, the marked increase in the oxygen atomic ratio confirmed the success of this oxidation method. Similarly to the oxidized NCD surface, the aminated NCD surface also exhibited an increase in oxygen contents but a smaller increase was observed than that of the directly oxidized surface. The higher oxygen atomic ratio (41.2%) on the oxidized NCD is probably related to the sufficient ozone content in the UV/ozone chamber. However, nitrogen gas was introduced to repel oxygen gas, and there was very limited oxygen source available as a source for direct amination. Therefore, the aminated surface has a lower content of oxygen (34.1%) than the surface subjected to direct oxidation. However, the amounts of these oxygen components are relatively high, especially compared with the amount of nitrogen atoms. The functionalization efficiencies of oxygen and nitrogen related groups on the NCD surface were markedly different, and much lower nitrogen-related groups were obtained than oxygen components. It is highly possible that the oxygen in the chamber affected the covalent binding of nitrogen-related components, and that the oxygen plays an important role in increasing the functionalizaiton of amine groups.[5,12] Compared with the hydrogenated surface, the fluorinated NCD surface had a smaller ratio of oxygen atoms, this may be closely related to the use of powerful fluorine plasma, which may substitute the fluorine-related terminations for oxygen terminations on the NCD surface.

**Table 2. Coverage of Functionalized Groups and the Contact Angle of Water on Hydrogenated, Aminated, Carboxylated, And Fluorinated NCD Films**

| NCD surface | atomic ratio O/C (%) | useful groups for biosensor | percentage (%) | wetting angle (deg) |
|---|---|---|---|---|
| hydrogenated | 2.2 | | | 92 |
| aminated | 34.1 | -$NH_2$ | 23 | 43 |
| carboxylated | 41.2 | -COOH | 12 | 23 |
| fluorinated | 1.8 | C−$F_x$ | 43 | 126 |

In addition, Table 2 also shows the functional groups that can be used in biosensor design and their densities. The density of different functional groups determines the effective number of probing aptamers that can be immobilized on the aminated and carboxylated NCD films, and therefore the performance of

the NCD biosensor. Compared with an NCD surface indirectly functionalized with carboxyl groups via linker molecules,[20] the density of directly covalently bonded carboxyl groups was similar and on the order of $1 \times 10^{14}$ molecules/cm$^{-2}$. In summary, for all the functional groups it was clearly shown that effective surface functionalization was successfully achieved on the NCD surface by introducing types of covalent bonds.

**Water Contact Angle Test.** Surface wettability was investigated by comparing the hydrophilicity/hydrophobicity difference between all the functionalized NCD films. Compared with the hydrogenated surface, the NCD films became much more hydrophilic after direct UV/ozone oxidation and photochemical amination, as evidenced by the results of contact angle test shown in Table 2. The UV/ozone treated NCD films were more hydrophilic than the directly aminated diamond, which can be attributed to the higher density of oxygen related functional groups on the UV/ozone-oxidized films. These differences in wettability are in reasonably good agreement with the XPS results in Figure 3, which also reveal a higher number of oxygen-related chemical groups on the oxidized NCD films than on the aminated diamonds. In contrast, the fluorinated NCD films display the highest contact angle against water molecules (126°), illustrating the super-hydrophobic characteristic of fluorinated NCD films. The hydrophobic surface can inhibit the attachment of biomolecules onto NCD films owing to the repulsive force provided by the fluorine-related chemical groups.

**Fluorescence Measurement.** The fluorescence intensity obtained using an epi-fluorescence microscope shown in Figures 5, 6, and 7 was normalized by the surface coverage of carboxyl (12%) and amine (23%) groups on the carboxylated and aminated NCD films used as biosensors, respectively. The background noise was subtracted in all the plots. Figure 5 shows the biosensor performance for PDGF protein detection in a wide range of concentrations from $1 \times 10^3$ nM to $1 \times 10^{-3}$ nM. It is clear that the relative fluorescence intensity decreases with decreasing concentration of PDGF introduced onto the NCD biosensors, implying their concentration-dependent sensitivity. The sensitivity of the directly functionalized NCD biosensors is high with strong fluorescence when PDGF protein with a concentration of $1 \times 10^3$ nM was introduced onto the biosensor. When the PDGF protein concentration was decreased to $1 \times 10^{-2}$ nM, the NCD biosensors still displayed reasonably strong fluorescence, implying a low detection limit. In a previous investigation, a PDGF detector was designed that employed a diamond transistor and was based on the charging of biomolecules by a current−voltage signal. However, it was difficult to obtain a low detection limit.[21] This demonstrates the higher sensitivity of NCD biosensors for PDGF protein detection than that on the previous method. In fact, the signal gain of an aptasensor is closely related to the surface coverage of probe aptamers that can be realized on the functionalized NCD surface. As mentioned above in the XPS observation, the number of effective probe aptamers immobilized on an aminated NCD surface can be increased for a carboxylated NCD biosensor surface by optimizing the oxidation method.[22]

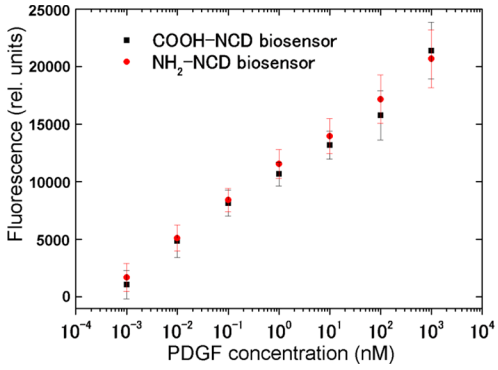


**Figure 5.** Biosensor sensitivity response for PDGF-BB detection in a wide concentration range of 1000 nM to 1 pM of NCD biosensors. The fluorescence intensity is normalized by the surface coverage of carboxyl (12%) and amine (23%) groups on the directly carboxylated and aminated NCD biosensors, respectively, and the background noise (approximately 7000 units) in the fluorescence intensity is subtracted in the plot.

In addition, a low detection limit that depends on the intensity of the signal can be expected varying the target PDGF protein concentration. The fluorescence intensity decreases evidently with decreasing PDGF protein concentration introduced onto the immobilized probes. Because the PDGF concentrations in the blood serum and plasma of normal individuals and cancer patients have been found to be in the subnanomolar range, 0.4−0.7 nM in human serum and 0.008−0.04 nM in human plasma,[23−25] the low limit of detection in the picomolar range achieved in the study indicates the potential of the NCD biosensor for clinical applications.

In addition to sensitivity, high selectivity is another important characteristic for evaluating the performance of a biosensor. We investigated the selectivity of the NCD biosensors against other biochemicals including ATP, glucose oxidase, urease, and calmodulin, as well as other PDGF isoforms such as PDGF-AA, PDGF-AB, and PDGF-BB variants, the result of which were shown in Figure 6a. The fluorescence behavior was investigated by evaluating the effectiveness of the immobilized biomolecules at a fixed concentration of 1000 nM. An extremely low fluorescence signal was obtained for ATP, glucose oxidase, urease and calmodulin, which were attributed to the inherent specific affinity of PDGF-binding aptamers to only PDGF proteins. However, the PDGF protein isoform PDGF-AB also exhibited a relatively strong fluorescence signal, which can be understood by considering the conformation structures of the proteins. Because PDGF proteins are composed of two monomers, A-chain and B-chain, three variants exist for PDGF proteins, PDGF-AA, PDGF-AB, and PDGF-BB. However, the PDGF binding aptamer only has very high specificity toward the PDGF-BB protein. For the variant PDGF-AB, an isoform with 60% similarity to PDGF-BB in its sequence of amino acids, half the intensity of the fluorescence signal was obtained compared with that of PDGF-B. In contrast, there was almost no fluorescence signal when the PDGF-AA variant was introduced onto the NCD biosensors. This major contrast in the intensity of the fluorescence signals is related to the biological conformation of these biomolecules, and the difference in fluorescence intensity confirmed the high selectivity of the NCD biosensors, even for the recognition of PDGF isoforms.

In addition, a selectivity investigation was carried out for BSA, which is a complex, contaminate matrix. The NCD biosensors were exposed for various amounts of BSA solution containing a fixed PDGF concentration ($1 \times 10^3$ nM), the results of which are shown in Figure 6b. The NCD biosensors did not show any degradation of the fluorescence intensity when exposed to the complex matrix, even in the case of a high

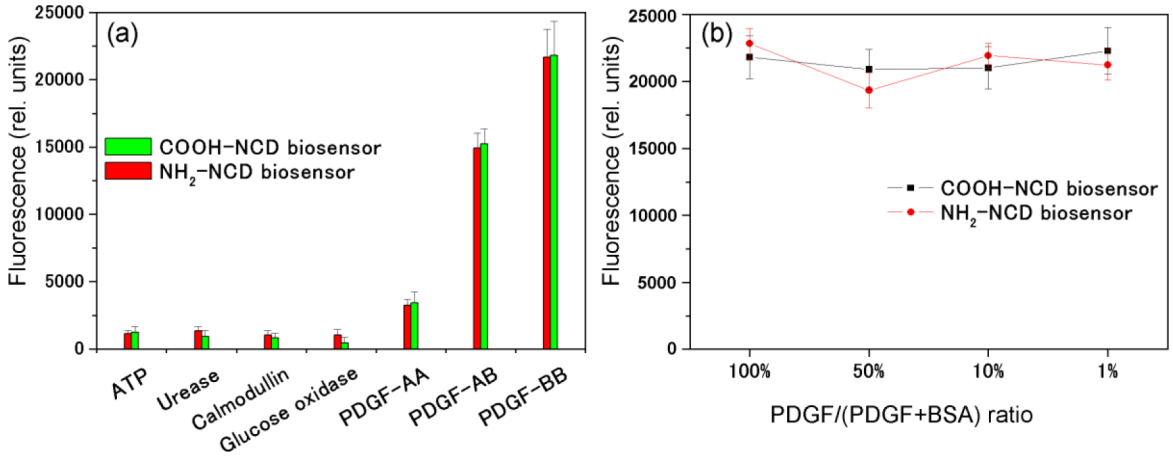


**Figure 6.** Selectivity of the NCD biosensors with surface functionalized by COOH and $NH_2$.

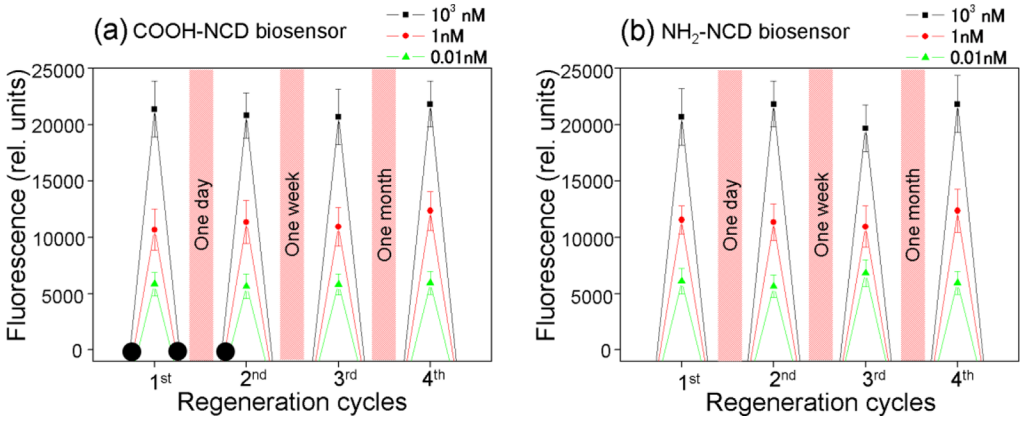


**Figure 7.** Stability and regeneration ability over time for NCD biosensors with functionalized with (a) COOH and (b) $NH_2$ used for PDGF detection.

concentration of serum proteins. The clearly distinguishable fluorescence signals confirm the high selectivity of the NCD biosensors in a complex environment containing serum proteins.

The stability of the NCD biosensors was investigated by evaluating their regeneration ability and lifetime. To effectively remove the PDGF proteins and Cy5-labeled aptamers, biosensor regeneration was performed using 10% sodium dodecyl sulfate (SDS) solution followed by thorough rinsing with DI water. After regeneration, the NCD sensors were stored in a refrigerator for lifetime testing. Figure 7 shows the regeneration performance of the NCD biosensors over time for PDGF concentrations of $1 \times 10^3$ nM, 1 nM, and 0.01 nM. It is noticeable that both the carboxylated and aminated NCD biosensors display high stability with distinguishable fluorescence intensity even after a month. When the concentration of PDGF introduced onto the NCD biosensors was decreased to 0.01 nM, the biosensors still clearly demonstrated excellent regeneration ability and high stability for PDGF detection in the long term test. The constant fluorescence intensity after 1 month exhibited by the NCD biosensors can be ascribed to the high stability of the NCD aptasensors against biofouling over a long lifetime. The high stability and reproducibility of the NCD biosensors reflect the high effectiveness of the chemical binding between the functionalized groups and the PDGF-binding aptamers, which also gives the NCD biosensor strong potential for use as a long-term reusable biosensor for clinical applications.

**Evaluation of Nonspecific Adsorption.** Nonspescific binding or adsorption can seriously degrade the biosensing performance of biosensor; therefore, many strategies have been applied to eliminate this negative effect. We also investigated nonspecific binding on the NCD biosensor surfaces, and evaluated the effect of such nonspecific adsorption on the NCD biosensors. The direct fluorescence signal obtained from the carboxylated NCD biosensor for the detection of $10^3$ nM PDGF detectionshown in Figure 8 was selected for a comparative investigation. The monochrome image in Figure 8a clearly shows strong fluorescence intensity of over $2 \times 10^4$ from the caboxylated NCD biosensor, and the fluorescence signal along the scanning lines is relatively constant around the maximum intensity, implying the uniform distribution of immobilized probing aptamers and conjugated PDGF proteins inside the patterned dots. Outside of the dots, the fluorescence intensity decreases to a level almost four times lower than that inside the dots. This can be attributed to the functionalization of the surface with fluorine resulting in superhydrophobic outside the dots, which can effectively prevent the physisorption of biomolecules in the vicinity. In Figure 8b, the patterns in pseudocolor form directly show the highly uniform intensity of the fluorescence signal inside of the dots, and the low intensity outside the dots; the signal color of fluorescence background also confirms the low signal noise on the


dx.doi.org/10.1021/am300595f | ACS Appl. Mater. Interfaces 2012, 4, 3526–3534

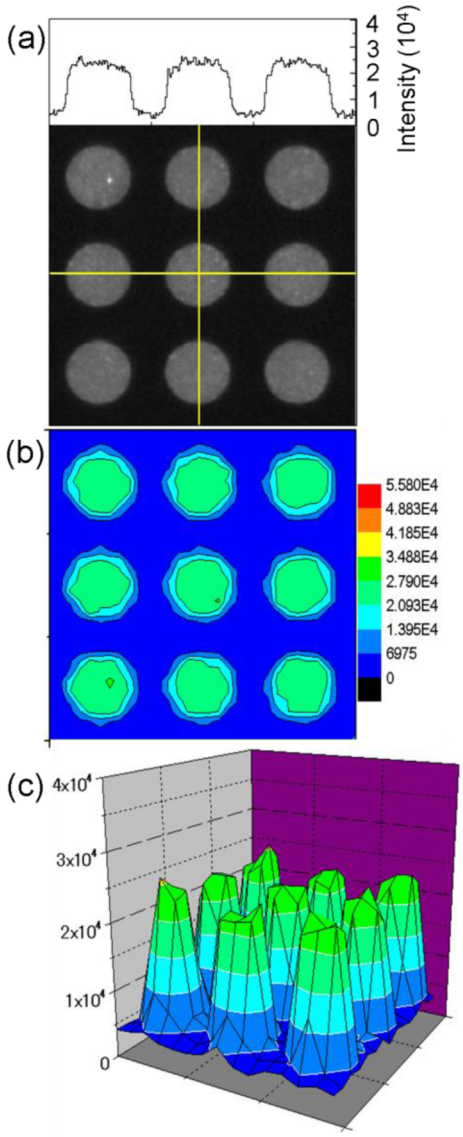


**Figure 8.** Fluorescence signal on carboxylated NCD biosensor.

carboxylated NCD biosensor surface. The graph in Figure 8c clearly shows that the fluorescence intensity is lower along the circumferences of the dots. This observation indicates that the carboxylated NCD surface can be used as a biosensing interface.

## CONCLUSIONS

Biosensors for PDGF detection fabricated on nanocrystalline diamond films were investigated using specific aptamers as recognition elements. XPS observations demonstrated that surfaces directly functionalized with carboxyl and amine groups provide comparable performance in immobilizing probe aptamers on the functionalized NCD films. Biosensors on directly carboxylated and aminated NCD films demonstrate high sensing performance in terms of sensitivity, selectivity, long-term stability, and regeneration ability, demonstrating that directly functionalized NCD films have the high potential to be used as effective sensing platforms. It is believed that NCD aptasensors will provide a new means combining directly functionalized NCD surfaces with versatile biomolecules.

## AUTHOR INFORMATION

### Corresponding Author

*E-mail: xianfen.wang@gmail.com.

### Notes

The authors declare no competing financial interest.

## ACKNOWLEDGMENTS

This research was supported by a Grant-in-Aid for Global Center of Excellence (GCOE) Research from the Ministry of Education, Culture, Sports, Science and Technology of Japan and a Grant-in-Aid for Fundamental Research A (23246069) from the Japan Society for the Promotion of Science (JSPS). Xianfen Wang gratefully appreciates the Chinese government for the China Scholarship Council Award.

## REFERENCES

(1) Yang, W. S.; Auciello, O.; Butler, J. E.; Cai, W.; Carlisle, J. A.; Gerbi, J.; Gruen, D. M.; Knickerbocker, T.; Lasseter, T. L.; Russell, J. N.; Smith, L. M.; Hamers, R. J. *Nat. Mater.* **2002**, *1*, 253−257.

(2) Hartl, A.; Schmich, E.; Garrido, J. A.; Hernando, J.; Catharino, S. C. R.; Walter, S.; Feulner, P.; Kromka, A.; Steinmuller, D.; Stutzmann, M. *Nat. Mater.* **2004**, *3*, 736−742.

(3) Notsu, H.; Yagi, I.; Tatsuma, T.; Tryk, D. A.; Fujishima, A. *Electrochem. Solid-State Lett.* **1999**, *2*, 522−524.

(4) Zhang, G. J.; Song, K. S.; Nakamura, Y.; Ueno, T.; Funatsu, T.; Ohdomari, I.; Kawarada, H. *Langmuir* **2006**, *22*, 3728−3734.

(5) Torrengo, S.; Miotello, A.; Minati, L.; Bernagozzi, I.; Ferrari, M.; Dipalo, M.; Kohn, E.; Speranza, G. *Diamond Relat. Mater.* **2011**, *20*, 990−994.

(6) Yang, J. H.; Song, K. S.; Zhang, G. J.; Degawa, M.; Sasaki, Y.; Ohdomari, I.; Kawarada, H. *Langmuir* **2006**, *22*, 11245−11250.

(7) Durrant, S. F.; Baranauskas, V.; Peterlevitz, A. C.; Castro, S. G.; Landers, R.; Bica de Moraes, M. A. *Diamond Relat. Mater.* **2001**, *10*, 490−495.

(8) Ray, M. A.; Tyler, T.; Hook, B.; Martin, A.; Cunningham, G.; Shenderova, O.; Davidson, J. L.; Howell, M.; Kang, W. P.; McGuire, G. *Diamond Relat. Mater.* **2007**, *16*, 2087−2089.

(9) Denisenko, A.; Romanyuk, A.; Pietzka, C.; Scharpf, J.; Kohn, E. *Surf. Sci.* **2011**, *605*, 632−637.

(10) Mascini, M. *Aptamers in Bioanalysis*, John Wiley & Sons: Hoboken, NJ, 2009.

(11) Tsugawa, K.; Ishihara, M.; Kim, J.; Koga, Y.; Hasegawa, M. *Phys. Rev. B: Condens. Matter Mater. Phys.* **2010**, *82*, 125460−125468.

(12) Torrengo, S.; Miotello, A.; Speranza, G.; Minati, L.; Bernagozzi, I.; Ferrari, M.; Chiasera, A.; Dipalo, M.; Kohn, E. *Adv. in Sci. Technol.* **2010**, *71*, 45−49.

(13) Fabisiak, K.; Maar-Stumm, M.; Blank, E. *Diamond Relat. Mater.* **1993**, *2*, 722−727.

(14) Williams, O. A. *Diamond Relat. Mater.* **2011**, *20*, 621−640.

(15) Beamson, G.; Briggs, D. *High Resolution XPS of Organic Polymers, The Scienta ESCA3000 Database*; Wiley: Chichester, U.K., 1992.

(16) Martin, H.; Argoitia, A.; Angus, J.; Landau, U. *J. Electrochem. Soc.* **1999**, *146*, 2959−2964.

(17) Ferro, S.; De Battisti, A. *Anal. Chem.* **2003**, *75*, 7040−7042.

(18) Kondo, T.; Kusakabe, K.; Ito, H.; Ohkawa, K.; Einaga, Y.; Fujishima, A.; Kawai, T. *Electrochim. Acta* **2007**, *52*, 3841−3848.

(19) Denisenko, A.; Romanyuk, A.; Pietzka, C.; Scharpf, J.; Kohn, E. *Diamond Relat. Mater.* **2010**, *19*, 423−427.

(20) Chong, K. F.; Loh, K. P.; Vedula, S. R. K.; Lim, C. T.; Sternschulte, H.; Steinschulte, D.; Sheu, F. S.; Zhong, Y. L. *Langmuir* **2007**, *23*, 5615−5621.

(21) Ruslinda, A. R.; Tajima, S.; Ishii, Y.; Ishiyama, Y.; Edgington, R.; Kawarada, H. *Biosens. Bioelectron.* **2010**, *26*, 1599−1604.

(22) Wang, X. F.; Hasegawa, M.; Tsugawa, K.; Ruslinda, A. R.; Kawarada, H. *Diamond Relat. Mater.* **2012**, *24*, 146−152.

(23) Singh, J. P.; Chaikin, M. A.; Stiles, C. D. *J. Cell Biol.* **1982**, *95*, 667−671.
(24) Bowen-Pope, D. F.; Malpass, T. W.; Foster, D. M.; Ross, R. *Blood* **1984**, *64*, 458−469.
(25) Leitzel, K.; Bryce, W.; Tomita, J.; Manderino, G.; Tribby, I.; Thomason, A.; Billingsley, M.; Podczaski, E.; Harvey, H.; Bartholomew, M.; Lipton, A. *Cancer Res.* **1991**, *51*, 4149−4154.